

## Mutations in *HOXD13* Underlie Syndactyly Type V and a Novel Brachydactyly-Syndactyly Syndrome

Xiuli Zhao,\* Miao Sun,\* Jin Zhao, J. Alfonso Leyva, Hongwen Zhu, Wei Yang, Xuan Zeng, Yang Ao, Qing Liu, Guoyang Liu, Wilson H. Y. Lo, Ethylin Wang Jabs, L. Mario Amzel, Xiangnian Shan, and Xue Zhang

*HOXD13*, the homeobox-containing gene located at the most 5' end of the *HOXD* cluster, plays a critical role in limb development. It has been shown that mutations in human *HOXD13* can give rise to limb malformations, with variable expressivity and a wide spectrum of clinical manifestations. Polyalanine expansions in *HOXD13* cause synpolydactyly, whereas amino acid substitutions in the homeodomain are associated with brachydactyly types D and E. We describe two large Han Chinese families with different limb malformations, one with syndactyly type V and the other with limb features overlapping brachydactyly types A4, D, and E and mild syndactyly of toes 2 and 3. Two-point linkage analysis showed LOD scores  $>3$  ( $\theta = 0$ ) for markers within and/or flanking the *HOXD13* locus in both families. In the family with syndactyly type V, we identified a missense mutation in the *HOXD13* homeodomain, c.950A→G (p.Q317R), which leads to substitution of the highly conserved glutamine that is important for DNA-binding specificity and affinity. In the family with complex brachydactyly and syndactyly, we detected a deletion of 21 bp in the imperfect GCN (where N denotes A, C, G, or T) triplet-containing exon 1 of *HOXD13*, which results in a polyalanine contraction of seven residues. Moreover, we found that the mutant *HOXD13* with the p.Q317R substitution was unable to transactivate the human *EPHA7* promoter. Molecular modeling data supported these experimental results. The calculated interactions energies were in agreement with the measured changes of the activity. Our data established the link between *HOXD13* and two additional limb phenotypes—syndactyly type V and brachydactyly type A4—and demonstrated that a polyalanine contraction in *HOXD13*, most likely, led to other digital anomalies but not to synpolydactyly. We suggest the term “*HOXD13* limb morphopathies” for the spectrum of limb disorders caused by *HOXD13* mutations.

The homeobox-containing (*HOX*) genes are a highly conserved transcription-factor family that displays important function in early development.<sup>1,2</sup> In humans, there are 39 *HOX* genes arranged in four separate clusters: *HOXA*, *HOXB*, *HOXC*, and *HOXD*.<sup>3</sup> These clusters are located on chromosomes 7p15, 17q21, 12q13, and 2q31, respectively, and show a striking colinearity in their 5'→3' genomic position and transcription direction. *HOXD13* (MIM \*142989; GenBank accession number NM\_000523), the most 5' gene of the *HOXD* cluster, has two coding exons: exon 1 with the imperfect GCN (where N denotes A, C, G, or T) triplet repeats encoding the N-terminal region with a 15-residue polyalanine tract (residues 49–63), and exon 2, which contains the homeobox region encoding the C-terminal portion with a 60-residue homeodomain (residues 268–327).<sup>4</sup> The homeodomain forms three  $\alpha$ -helices. Structural studies of *HOX* proteins have shown that residues in the recognition helix-3—mainly, the 47th isoleucine (I47), the 50th glutamine (Q50), and the 51st asparagine (N51) of the homeodomain—make base-specific DNA contacts in the major groove, and residues in the N-terminal arm in-

teract with the minor groove of DNA, thereby collaboratively determining DNA-binding specificity and affinity.<sup>5–10</sup>

*HOXD13* is the first *HOX* gene known to be linked to human developmental disorders.<sup>11,12</sup> Mutations in *HOXD13* are associated with limb deformities in both humans and mice, suggesting a critical role in limb development. Synpolydactyly (SPD [MIM 186000], or syndactyly type II) is a dominantly inherited limb malformation with incomplete penetrance and variable expressivity. It is characterized by soft-tissue syndactyly between fingers 3 and 4 and between toes 4 and 5, with partial or complete digit duplication within the syndactylous web. Both interfamilial and intrafamilial variations in SPD limb phenotype exist. Individuals with an atypical form of SPD share a distinctive set of foot phenotypes, including small spurs of bone between metatarsals 1 and 2.<sup>11</sup> Polyalanine-expansion mutations in *HOXD13* lead to typical SPD, whereas deletions and missense mutations are associated with atypical SPD.<sup>11–21</sup> Furthermore, in the spontaneous *spdh* mouse mutant, which has a phenotype similar to human SPD, a polyalanine expansion of seven residues in *Hoxd13* was de-

From the Department of Medical Genetics and National Key Laboratory of Medical Molecular Biology, Institute of Basic Medical Sciences, Chinese Academy of Medical Sciences and Peking Union Medical College, Beijing (X. Zhao; M.S.; J.Z.; W.Y.; X. Zeng; Y.A.; Q.L.; G.L.; W.H.Y.L.; X. Zhang); Genetics Research Center, Southeast University School of Medicine, Nanjing, China (X. Zhao; X.S.); Institute of Genetic Medicine, Center for Craniofacial Development and Disorders, The Johns Hopkins University (M.S.; E.W.J.), and Department of Biophysics and Biophysical Chemistry, The Johns Hopkins University School of Medicine (J.A.L.; L.M.A.), Baltimore; Center for Genetic Medicine, Lanzhou University, Lanzhou, China (H.Z.); and The Research Center for Medical Genomics, China Medical University, Shenyang, China (X. Zhang)

Received September 29, 2006; accepted for publication November 22, 2006; electronically published January 3, 2007.

Address for correspondence and reprints: Dr. Xue Zhang, Department of Medical Genetics, Institute of Basic Medical Sciences, Chinese Academy of Medical Sciences and Peking Union Medical College, 5 Dong Dan San Tiao, Beijing 100005, China. E-mail: xuezhang@pumc.edu.cn

\* These two authors contribute equally to this work.

*Am. J. Hum. Genet.* 2007;80:361–371. © 2007 by The American Society of Human Genetics. All rights reserved. 0002-9297/2007/8002-0017\$15.00

tected.<sup>22,23</sup> Missense mutations in *HOXD13* also underlie brachydactyly types D (BDD [MIM 113200]) and E (BDE [MIM 113300]).<sup>24,25</sup> BDD presents with short and broad distal phalanges of the thumbs and halluces, whereas BDE has the cardinal feature of one or more shortened metacarpals and/or metatarsals. Two *HOXD13* missense mutations within the homeodomain—p.S308C and p.I314L—have been described in families exhibiting features of BDE with BDD and BDE with mild SPD, respectively.<sup>24,25</sup>

Syndactyly type V (MIM 186300), defined as “syndactyly associated with metacarpal and metatarsal synostosis” by Temtamy and McKusick,<sup>26(p302)</sup> represents one of the rarest types of nonsyndromic syndactyly.<sup>27</sup> It is inherited as an autosomal dominant trait with synostotic fusion of metacarpals 4 and 5 as the hallmark.<sup>28</sup> Brachydactyly type A4 (BDA4 [MIM 112800]) is characterized by short middle phalanges of the 2nd and 5th fingers and absence of middle phalanges of the 2nd–5th toes. In this report, we describe limb phenotypes of syndactyly type V and a novel brachydactyly-syndactyly syndrome that includes BDA4, and we report novel mutations in *HOXD13* in two large Han Chinese families.

**Clinical findings.**—We investigated two large Han Chinese families with distinctive limb malformations. Both families had affected females and male-to-male transmission (fig. 1A and 1B), consistent with autosomal dominant inheritance. There were 23 affected individuals in the 6 generations of family 1 (fig. 1A). At the proband’s request, 13 affected individuals were physically examined, and digital photographs were taken. Among those individuals, 11 had hand and foot radiographs. On radiological examination, nine affected individuals had bilateral or unilateral fusion of metacarpals 4 and 5 (fig. 2B, 2F, 2J, and 2N). Radiographs showed that the fusion was variable in extent. The proband had a complete fusion in his right hand (fig. 2B), and eight other affected individuals had bilateral complete fusion (fig. 2F, 2J, and 2N). In five affected individuals, the fusion extended to the phalanges of fingers 4 and 5 (fig. 2N). Other hand deformities included ulnar deviation of fingers 2–5 (12 of 13 subjects), lobster claw-like or Y-shaped fingers 4 and 5 with an angulated 5th finger (8 of 13), shortening or clinodactyly of the 5th fingers (3 of 13), short distal phalanges of between one and all fingers (12 of 13), shortening of fused metacarpals 4 and 5 or metacarpal 5 (6 of 13), unilateral cutaneous syndactyly of fingers 3 and 4 (4 of 13), interdigital clefts between fingers 3 and 4 (10 of 13), camptodactyly (10 of 13), and absence of distal interphalangeal creases (13 of 13) (fig. 2A, 2B, 2E, 2F, 2I, 2J, 2M, and 2N). None of the affected individuals had metatarsal fusion of the feet (fig. 2D, 2H, 2L, and 2P). The most constant foot deformities were varus deviation of the first metatarsals; valgus deviation of toes 1–4; hyperplasia of the 1st ray, affecting the first metatarsals and the phalanges of the halluces; hypoplasia and shortness of metatarsals 2–5; and shortened and tucked 5th toes (fig. 2C, 2D, 2G, 2H, 2K, 2L, 2O, and 2P). Mild cutaneous syndactyly of toes 2 and 3 or 3 and 4 was

observed in four affected individuals (IV-5, IV-8, IV-10, and V-13) (fig. 2K). Of note, one affected individual (V-9) with bilateral complete fusion of metacarpals 4 and 5 also had postaxial polydactyly in his left hand, as well as hypospadias. Taken together, the phenotypes in this family closely resemble the syndactyly type V reported by Robinow and colleagues.<sup>28</sup>

Family 2 also had 23 affected individuals in 6 generations (fig. 1B). All 17 patients who are still alive were available for phenotype evaluation. Digital photographs and radiographs were taken for 16 and 13 of them, respectively. On clinical examination, most of the patients exhibited generalized shortening of hands and feet, 11 displayed broad and short distal phalanges of the thumbs (fig. 3A, 3E, 3I, and 3M), and 14 had mild cutaneous syndactyly of toes 2 and 3 (fig. 3C, 3G, 3K, and 3O). Radiographs revealed a constant phenotypic feature in all 13 patients: absence of middle phalanges of toes 2–5 (fig. 3D, 3H, 3L, and 3P) and very marked short middle phalanges of the 5th finger (fig. 3B, 3F, 3J, and 3N). Combined shortening of the middle phalanges was noticed, with patterns 2–5 (3 patients), 2-4-5 (3 patients), and 2-3-4-5 (2 patients), which indicates that the 2nd and 5th fingers are most severely affected (fig. 3B, 3F, 3J, and 3N). In many cases, the shortened middle phalanges were fused with the distal ones (fig. 3B, 3F, 3J, and 3N). In 12 patients, radiographs also showed very pronounced shortening of metacarpal 5, either alone or in combination with metatarsal 5 and/or other metacarpals/metatarsals (fig. 3B, 3D, 3F, 3H, 3J, 3L, 3N, and 3P). Short proximal phalanges of toes 1, 3, and 4 were apparent in 7 patients (fig. 3H, 3L, and 3P). Other common limb anomalies included broad first metatarsals and hallux phalanges, often associated with hallux valgus (fig. 3C, 3D, 3G, 3H, 3K, 3L, 3O, and 3P). Notably, the proband also had small spurs of bone between the 1st and 2nd metatarsals (fig. 3D). Almost all limb anomalies in this family were bilateral. These limb phenotypes overlap with those of BDA4, BDD, and BDE, and syndactyly type I (MIM %185900). No family member showed short stature or polydactyly.

**Molecular genetics.**—We performed two-point linkage analysis and mutation identification after obtaining informed consent from participating family members and approval of Peking Union Medical College Institutional Review Board. Blood samples were collected and genomic DNA was extracted from 27 members of family 1, including 13 patients, and from 43 family members of family 2, including 15 patients. Six polymorphic microsatellite markers from chromosome region 2q24.3-q32.1, including a CA-repeat sequence within the intron of the *HOXD13* gene, were selected and typed in the families, for two-point linkage analysis. LOD scores were calculated using the MLINK program of the LINKAGE package. The parameters used in linkage analysis were autosomal dominant inheritance, complete penetrance, a mutation rate of zero, equal male-female recombination rate, equal microsatellite-allele frequency, and a disease-allele frequency of 1

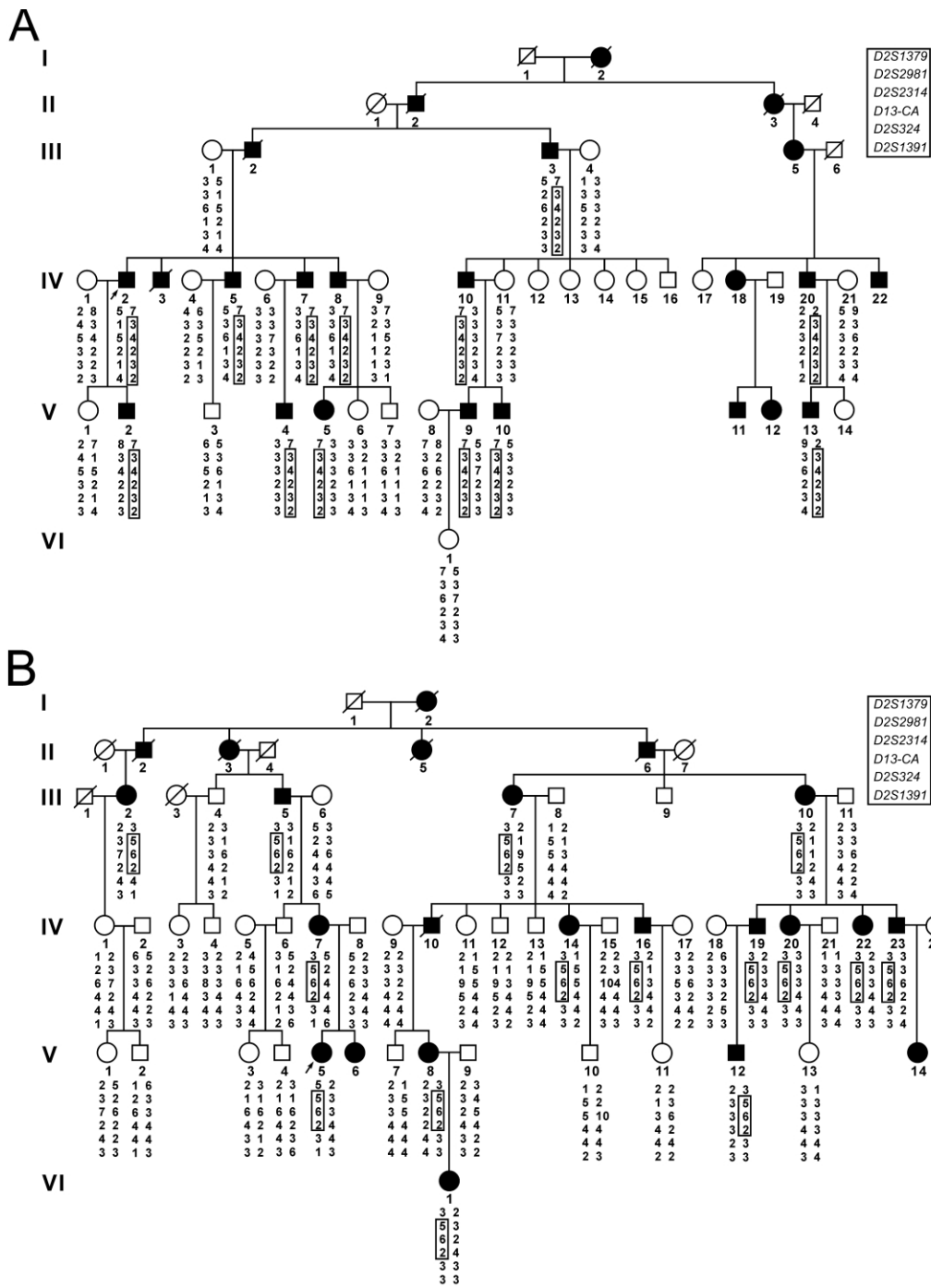


**Figure 1.** Pedigrees and disease-haplotype segregation of family 1 (A) and family 2 (B). Blackened symbols represent affected individuals with abnormal limb phenotype, and unblackened symbols represent individuals with a normal limb phenotype. Circles and squares indicate females and males, respectively. The arrows identify the probands. The disease haplotype is boxed.

in 10,000. Maximal LOD scores of 4.90 in family 1 and of 6.46 in family 2 were obtained for marker *D2S2314* at  $\theta = 0.00$ , showing definitive evidence of linkage. Haplotype analysis indicated no recombination at five genetic markers (*D2S2981*, *D2S2314*, *D13-CA*, *D2S324*, and *D2S1391*) in family 1 (fig. 1A) and 3 markers (*D2S2981*, *D2S2314*, and *D13-CA*) in family 2 (fig. 1B), indicating

that the disease locus was linked to the chromosome region harboring *HOXD13*. We searched for pathogenic mutations in the proband of family 1 by direct sequencing of the PCR-amplified DNA fragments spanning exons 1 and 2 of *HOXD13*. We identified a missense mutation, c.950A→G (p.Q317R), substituting an arginine (R) for the highly conserved Q50, which is important for DNA-bind-



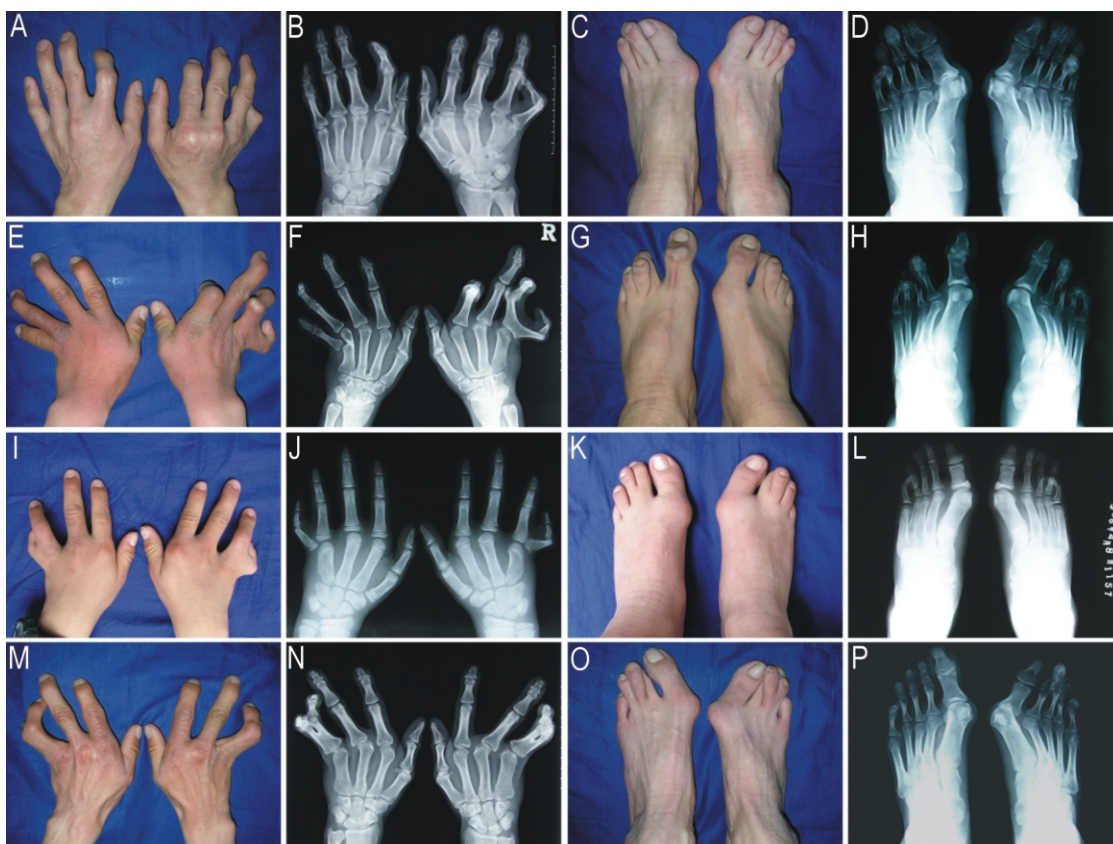


**Figure 2.** Photographs and radiographs of the proband (A–D), individual V-10 (E–H), individual V-13 (I–L), and individual IV-10 (M–P) of family 1.

ing specificity and affinity (fig. 4A). To confirm this missense mutation, we introduced into the 950G mutant allele a *Bam*HI recognition sequence (5'-GGATCC-3'), using a mismatch primer (5'-CTTGTCTTCACTCTTCGGATC-3') in a semi-nested PCR. Restriction analysis with use of this *Bam*HI site in all available members from family 1 and in 136 unrelated control individuals of similar ethnic background revealed the presence of the mutation in all affected individuals but not in unaffected family members and control individuals (fig. 4A). In the proband of family 2, we sequenced the entire *HOXD13* gene, including a promoter region of 1.5 kb, two exons, one intron, two UTRs (5'-UTR and 3'-UTR), and the coding exons of *HOXD9* (GenBank accession number NM\_014213), *HOXD10* (GenBank accession number NM\_002148), *HOXD11* (GenBank accession number NM\_021192), and *HOXD12* (GenBank accession number NM\_021193). We found a deletion of 21 bp in the imperfect GCN triplet-repeat sequence of *HOXD13* exon 1, c.157\_177del, which results in a polyalanine contraction of seven residues (p.A53\_A59del) (fig. 4B). By polyacrylamide gel electrophoresis, it was confirmed that this deletion cosegregated with the limb phenotypes in affected individuals but was not detected in any unaffected individuals of the family or in 500 unrelated Han Chinese control individuals. A 4-alanine con-

traction was detected in the control individuals, with an allele frequency of 0.3% (3 in 1,000). We also identified a novel missense mutation in *HOXD11*—c.734G→A (p.G245D)—on the same chromosome that carries the 7-alanine contraction mutation in *HOXD13*. This *HOXD11* mutation was detected in 2 of 139 unrelated Han Chinese control individuals.

**Functional study.**—We conducted the luciferase reporter assay to determine the consequences of the p.Q317R substitution in transactivating the promoter of *EPHA7* (GenBank accession number NM\_004440), one of the direct downstream target genes of *HOXD13* during limb development.<sup>29</sup> The p.I314L and p.Q317R mutations in *HOXD13* change the amino acids at the 47th and 50th residues of the homeodomain, respectively. "I47L" had been used elsewhere to designate the p.I314L mutation.<sup>25</sup> Similarly, we named the mutant *HOXD13* with the p.Q317R substitution "Q50R." The human *EPHA7* promoter of 660 bp (from -580 to +80), which contains an *HOXD13*-binding site ATATTATGG, was obtained by PCR from human genomic DNA through use of primers EPHA7BamF 5'-CGCGGATCCTGTTCGCTCGCACCGT-3' and EPHA7R 5'-AGACTTCCTTCCCCTCCC-3'. The amplified fragment was cloned into the pGL3-basic vector (Promega) at the *Bgl*III and *Kpn*I sites upstream of the firefly luciferase gene and was verified



**Figure 3.** Photographs and radiographs of the proband (A–D), individual III-10 (E–H), individual IV-19 (I–L), and individual IV-23 (M–P) of family 2.

by sequencing (fig. 5A). To make the expression vectors for FLAG-HOXD13<sup>WT</sup> (the FLAG-tagged wild type) and FLAG-HOXD13<sup>-7A</sup> (the FLAG-tagged mutant with the 7-alanine contraction), the full coding regions were generated by genomic PCR from normal and affected individuals, respectively. The verified fragments were then cloned into the *Hind*III and *Sma*I sites of the p3 × FLAG-CMV-7 plasmid (Sigma), to produce the pFLAG-HOXD13<sup>WT</sup> and pFLAG-HOXD13<sup>-7A</sup> expression vectors, respectively. pFLAG-HOXD13<sup>Q50R</sup> and pFLAG-HOXD13<sup>I47L</sup> were constructed from the pFLAG-HOXD13<sup>WT</sup> by site-directed mutagenesis with use of the QuikChange Site-Directed Mutagenesis Kit (Stratagene). The primer pairs used were 5'-CCATTTGGTTTCGGAACCGAAGAGTG-3' and 5'-CACTC-TTCGGTTCGGAACCAAATGG-3' for Q50R and 5'-GACA-AGTGACCCTTTGGTTTCAG-3' and 5'-CTGAAACCAAAGG-GTCACTTGTC-3' for I47L. The reporter construct (1.0 μg) was cotransfected with 1.5 μg of one of the four test constructs (pFLAG-HOXD13<sup>WT</sup>, pFLAG-HOXD13<sup>Q50R</sup>, pFLAG-HOXD13<sup>I47L</sup>, or pFLAG-HOXD13<sup>-7A</sup>) into the C3H10T1/2 mouse embryonic fibroblast cells growing in a 12-well plate, with use of 1.0 μl VigoFect reagent (Vigorous Biotechnology). The pRL-SV40 *Renilla* luciferase vector (25 ng) was also added in each cotransfection, to normalize the transfection efficiency. Cells were lysed and assayed for luciferase activity following the Dual Luciferase protocol (Promega). Consistent with the recent findings that the mouse *Epha7* promoter could mediate transcriptional

activation by HOXD13, expression of the human wild-type HOXD13<sup>WT</sup> could also transactivate the human *EPHA7* promoter (fig. 5B).<sup>29</sup> However, a remarkable difference in the decrease of transactivation between the HOXD13<sup>Q50R</sup> and HOXD13<sup>I47L</sup> mutants was observed (fig. 5B and 5C). Q50R more severely impaired HOXD13's capacity to transactivate the human *EPHA7* promoter, retaining only 13% of the reporter activity compared with the wild-type counterpart, whereas I47L showed merely moderate impairment, with 63% of reporter activity remaining (fig. 5C). The polyalanine contraction of seven residues seemed to exert no significant effect on HOXD13-induced transactivation (fig. 5B and 5C). Cotransfection of pFLAG-HOXD13<sup>WT</sup> and pFLAG-HOXD13<sup>-7A</sup> showed no significant change in transcriptional activity (data not shown).

**Molecular modeling.**—We modeled the interaction between the Q50R-mutant HOXD13 and DNA on the basis of the crystal structure of *Drosophila melanogaster antenna-pedia* (*antp*) homeodomain (Protein Data Bank ID 9ANT) bound to DNA (fig. 6A). The Antp/DNA complex (PDB ID: 9ANT) was used as template for the modeling experiments.<sup>30</sup> I47 and Q50 of the homeodomain are identical in 9ANT and HOXD13. The base corresponding to the 3'-thymidine (Thy) in the core DNA consensus sequence 5'-TAAT-3' is Thy221 in 9ANT. To study the role of residues 47 and 50 of the HOXD13 homeodomain and the interacting base (Thy), four models in the protein-DNA inter-





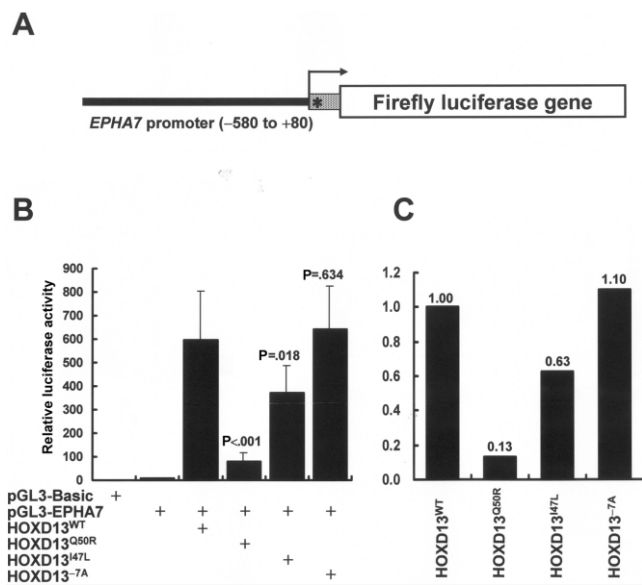


**Figure 5.** Transcriptional activity of wild-type and mutant HOXD13 proteins at the human *EPHA7* promoter. *A*, Schematic diagram of the reporter construct used in transfection assays. *B*, Transcriptional activity mediated by HOXD13<sup>WT</sup>, HOXD13<sup>Q50R</sup>, HOXD13<sup>I47L</sup>, and HOXD13<sup>-7A</sup>. Bars represent firefly/*Renilla* luciferase ratios for the different constructs. Values are the means ( $\pm$  SEM) of eight independent experiments. The significance of differences in expression was calculated using the independent-samples *T* test. *P* values are presented above the bars. *C*, Relative decrease of transcriptional activity mediated by mutant HOXD13 proteins compared with the wild-type HOXD13<sup>WT</sup>.

BDE with mild SPD caused by p.I314L,<sup>24,25</sup> syndactyly type V caused by p.Q317R, and BDA4/BDD/BDE with mild 2–3 toe syndactyly caused by a polyalanine contraction.

Syndactyly type V, as a distinct entity, has 4–5 metacarpal synostosis, a cardinal feature distinguishing it from other nonsyndromic syndactylies.<sup>27,28</sup> Study of family 1, a 6-generation Chinese family affected with this rare limb malformation, enabled us to map the disease locus to the chromosomal region where *HOXD13* is located. In this Han Chinese family, we identified a missense mutation of *HOXD13*—c.950A→G (p.Q317R)—that substituted the basic and charged polar amino acid R for the uncharged polar Q at the 50th residue of the homeodomain (Q50). This mutation was found to cosegregate with the disease phenotype in the large family but not was present in any unaffected family members or in 136 normal Han Chinese control individuals. Q50 of the homeodomain is invariant in all known HOX proteins (Homeodomain Resource) and has been shown to be a key amino acid for DNA-binding specificity and affinity.<sup>5–10,37</sup> Moreover, our functional study showed that the mutation had a deleterious effect on HOXD13-induced transcriptional activation of the human *EPHA7* promoter. Finally, molecular modeling data supported the in vitro experimental results. All these

results established conclusively the pathogenicity of the c.950A→G (p.Q317R) mutation in syndactyly type V.

SPD was the first disease in which polyalanine expansion was identified as the disease-causing mechanism.<sup>12</sup> This novel type of mutation has been found in nine different human genetic diseases.<sup>38–40</sup> Like *HOXD13* in SPD, polyalanine expansions in these genetic diseases show meiotic stability over generations, distinguishing it from dynamic triplet-repeat expansions underlying genetic diseases such as Huntington disease and fragile X syndrome. Unequal crossing-over has been suggested as the mechanism for polyalanine expansion.<sup>41</sup> Polyalanine contraction, the reciprocal allele of this unequal crossing-over, has not previously been associated with a human genetic disease,<sup>39</sup> although Dr. Stephen T. Warren has predicted that the mutant *HOXD13* alleles with truncated polyalanine tracts of fewer than eight residues “might lead to other digital anomalies.”<sup>41(p408)</sup> In the large Han Chinese family affected with combined BDA4/BDD/BDE and mild 2–3 toe syndactyly, we mapped the disease locus to a chromosome region defined by *D2S1379* and *D2S324* (fig. 1B). This region contains >70 known genes, including the 9 *HOXD* genes (Human Genome Browser Gateway). We sequenced all the 5' *HOXD* genes that show expression in the limb bud<sup>42</sup> and found a polyalanine contraction of seven residues in HOXD13 that segregated perfectly with the digital anomalies. The contraction was not detectable in 500 unrelated and ethnically matched unaffected control individuals. The site and length of the polyalanine tract in HOXD13, like that in the paralogous HOXA13, are highly conserved among mammals.<sup>43</sup> All mammalian HOXD13 proteins with sequences available in the databases—including human, chimpanzee, mouse, rat, and bat—have a 15-residue polyalanine tract in their N-terminal region, which suggests a strong functional and structural constraint. It has been indicated that a polyalanine tract beyond a certain threshold will have deleterious effects.<sup>40</sup> Mutations in *HOXD13* have been associated with BDD and BDE, whereas mild 2–3 toe syndactyly is common in individuals heterozygous for a 7-alanine expansion mutation in *HOXD13*.<sup>13,24</sup> Furthermore, homozygous mouse mutants with the disrupted *Hoxd13* gene showed absence of the second phalanges in digits II and V, size reduction of the second phalanges in digits III and IV, deformed and thicker metatarsal I with anterior protrusion, and shortened metacarpals and metatarsals in both of the forelimbs and the hindlimbs.<sup>44,45</sup> These, taken together, suggested that the 7-alanine contraction mutation in *HOXD13* was most likely responsible for the novel brachydactyly-syndactyly syndrome. In unaffected individuals, other researchers have detected 2- and 4-alanine contractions in HOXD13.<sup>16,46</sup> In our Han Chinese control individuals, the 4-alanine contraction reported<sup>46</sup> elsewhere in the Japanese population was detected as a very rare allele. Several other genes with pathogenic polyalanine expansions also display polyalanine tract-length polymorphisms—that is, expansions and contractions—in the general population.<sup>39</sup>

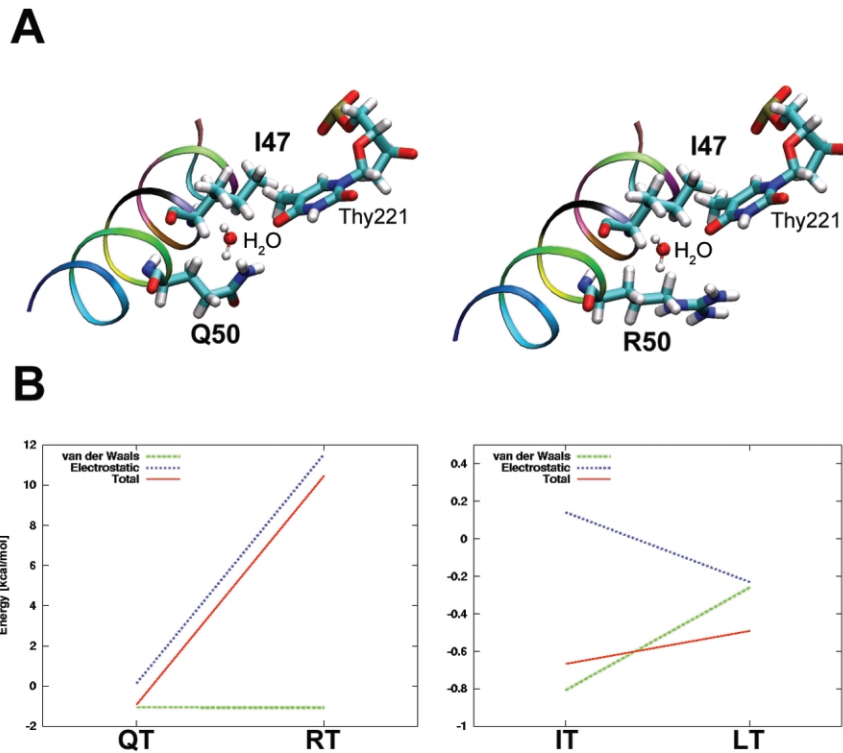


**Figure 6.** Interaction between HOXD13 and DNA. *A*, Models based on the Antp/DNA complex. The DNA is color coded as follow: carbon = cyan; oxygen = red; nitrogen = dark blue; phosphate = gold. For the helix III of the homeodomain, the main chain is represented, and only the side chains of the I47 and Q50 (*left panel*) and of the I47 and R50 (*right panel*) are drawn. *B*, Total (*red line*), electrostatic (*blue line*), and van der Waals (*green line*) interactions energies (in kcal/mol) between Q50 and Thy (wild type) and between R50 and Thy (mutant) (*left panel*) and between I47 and Thy (wild type) and L47 and Thy (mutant) (*right panel*). The numbers 47 and 50 represent the position of the amino acid in the homeodomain.

<sup>47</sup> Therefore, polyalanine contraction of fewer than seven residues in HOXD13, as in the case of polyalanine expansion, might represent polymorphisms and might not be pathogenic. Noticeably, a novel missense mutation in *HOXD11* (c.734G→A), substituting the acidic aspartate (D) for the nonpolar glycine (G) at residue 245 (p.G245D), was found in all affected individuals in the family. This substitution was also detected in unaffected controls. In mice and chickens, digit I identity was assumed to be *Hoxd13* positive and *Hoxd12/Hoxd11* negative.<sup>48</sup> Affected individuals in family 2, however, frequently showed deformed thumbs and halluces (digit I). Moreover, the hindlimbs of *Hoxd11*<sup>-/-</sup> mice showed no major defects, although the forelimbs displayed a strong reduction in length of the second phalanges in digits II and V and shortened metacarpals.<sup>49</sup> Therefore, the missense mutation in *HOXD11* might represent a rare polymorphism.

HOXD13 limb morphopathies cover several distinctive sets of limb malformations with different pathogenic mechanisms. Studies of mice (*Hoxd13*<sup>-/-</sup>/*Hoxd12*<sup>-/-</sup>/*Hoxd11*<sup>-/-</sup> knockout and *spd* mutant), mammalian cells, and clinical SPD cases have suggested a “super” dominant negative effect as the pathogenic mechanism underlying typical SPD.<sup>13,16,50–52</sup> Molecular analysis of different families has

indicated that loss-of-function mutations in *HOXD13* lead to atypical SPD.<sup>18–21</sup> Recently, *Hoxd13* has been shown to be a regulator of *Epha7* during limb development.<sup>29</sup> Both human HOXD13 and mouse *Hoxd13* can directly bind to a regulatory element within the *Epha7* promoter. Ectopic expression of HOXD13 in mouse cells can activate transcription of the endogenous *Epha7* gene and transactivate the *Epha7* promoter in a reporter construct. In contrast, the mutant HOXD13 with I47L does not bind to the regulatory element and induces only a minor transactivation of the *Epha7* promoter.<sup>29</sup> The syndactyly type V described in our present report and the work of Robinow et al.<sup>28</sup> had a common limb feature with atypical SPD: hyperplasia of the 1st ray in feet displayed as unusually broad hallux phalanges and first metatarsals.<sup>28</sup> Using a luciferase reporter construct containing the human *EPHA7* promoter, we showed that Q50R exerted much more severe impairment in HOXD13-induced transactivation and that the HOXD13<sup>I47L</sup> mutant retained considerable activity, which suggests a complete loss of function for HOXD13<sup>Q50R</sup> and a partial loss of function for HOXD13<sup>I47L</sup> in regulation of *EPHA7*, respectively. The difference in transactivation provided a molecular basis for the different limb phenotypes produced by these two mutations. However, metacarpal



fusions in syndactyly type V could be a gain-of-function effect, because this limb phenotype was absent both in patients with atypical SPD and in *Hoxd13* knockout mice.<sup>4,12–17,44,45</sup> It has been demonstrated elsewhere<sup>9,10</sup> that Q50 is an important determinant of differential DNA-binding specificity among different homeodomains. A single amino acid substitution to the basic and charged polar lysine (K) could switch the DNA-binding specificities of different homeodomains.<sup>9,10</sup> Guttmacher syndrome (MIM 176305) shares some phenotypes with hand-foot-genital syndrome (MIM 140000), which is caused by loss-of-function mutations in *HOXA13*.<sup>53</sup> In patients affected with Guttmacher syndrome, the p.Q371L missense mutation was identified.<sup>54</sup> This mutation led to a substitution at Q50 of the *HOXA13* homeodomain. The presence of additional limb phenotypes in Guttmacher syndrome suggested that the amino acid substitution resulted in both a loss and specific gain of function.<sup>54</sup> It is conceivable that a mixed gain and loss of function of *HOXD13*<sup>Q50R</sup> is a reasonable explanation of the cause of syndactyly type V. The polyalanine contraction found in the family with BDA4/BDD/BDE and mild 2–3 toe syndactyly is more likely a dominant-negative mutation, since *Hoxd13*<sup>-/-</sup> mice have similar phalangeal and metacarpal/metatarsal defects.<sup>44,45</sup> Transheterozygous *Hoxd13*<sup>-/+</sup>/*Hoxd12*<sup>-/+</sup> mice also exhibit a reduction of digits II and V in the forelimbs.<sup>44</sup> Furthermore, hypoplasia of the middle phalanges of toes 2–5 and broad hallux phalanges and first metatarsals are consistent in atypical SPD associated with functional haploinsufficiency for the homeodomain of *HOXD13*.<sup>18–21</sup> However, our reporter assay showed no significant difference between *HOXD13*<sup>WT</sup> and *HOXD13*<sup>-7A</sup> in regulation of *EPHA7*. Mutant *HOXD13* proteins with polyalanine tracts longer than 22 residues displayed misfolding and cytoplasmic aggregation.<sup>40</sup> We observed that the GFP-tagged *HOXD13* proteins with different polyalanine contractions were all located in the nucleus (data not shown). Polyalanine tracts are common in transcription factors and may modulate transcriptional regulation and protein-protein interaction.<sup>38,47</sup> Interestingly, longer polyalanine tracts (>10 alanines) formed  $\beta$ -sheet, whereas shorter ones (7 alanines) adopted  $\alpha$ -helix exclusively.<sup>55</sup> It is possible that the 7-alanine contraction in *HOXD13* could perturb its binding to the cofactors or trigger a rapid protein processing.

Our present report and the observations of others all indicate the existence of genotype-phenotype correlation for the limb morphopathies caused by *HOXD13* mutations.<sup>11,13,16,24</sup> However, the same minor malformations may be associated with the different limb clinical abnormalities—for example, (1) soft-tissue syndactyly of toes 2 and 3 in mild SPD due to a polyalanine expansion of seven residues, in the brachydactyly-syndactyly syndrome caused by a polyalanine contraction of seven residues, and in syndactyly type V, and (2) cutaneous syndactyly of fingers 3 and 4 without digit duplication within the web in mild SPD and syndactyly type V. Therefore, different limb

malformations due to distinct classes of *HOXD13* mutations should be considered a continuum of phenotypes.

## Acknowledgments

We are grateful to Drs. Yan Shen, Depei Liu, and Boqin Qiang for their encouragement and support. We thank all the family members for their generous participation. This work was supported by the National 863 Program of China, the National Natural Science Foundation of China Funds for Creative Research Groups grant 30421003, Distinguished Young Scholars grant 30125017, and China Medical Board of New York grant 03-785 (all to X. Zhang). J.A.L. was supported by National Institutes of Health (NIH) grant GM 066895 (to L.M.A.). M.S., Y.A., and X. Zhang are trainees in the International Collaborative Genetics Research Training Program (supported by NIH grant D43 TW06176). We also thank Dr. Depei Liu's group for technical assistance in functional study and Drs. Qi Xu and Ying Liu for providing DNA samples from unrelated Han Chinese individuals.

## Web Resources

Accession numbers and URLs for data presented herein are as follows:

GenBank, <http://www.ncbi.nlm.nih.gov/Genbank/> (for *HOXD13* [accession number NM\_000523], *HOXD9* [accession number NM\_014213], *HOXD10* [accession number NM\_002148], *HOXD11* [accession number NM\_021192], *HOXD12* [accession number NM\_021193], and *EPHA7* [accession number NM\_004440])

Homeodomain Resource, <http://genome.nih.gov/homeodomain/>  
Human Genome Browser Gateway, <http://genome.ucsc.edu/cgi-bin/hgGateway>

Online Mendelian Inheritance in Man (OMIM), <http://www.ncbi.nlm.nih.gov/Omim/> (for *HOXD13*, SPD, BDD, BDE, syndactyly type V, BDA4, syndactyly type I, Guttmacher syndrome, and hand-foot-genital syndrome)

Protein Data Bank, <http://www.rcsb.org/pdb/> (for the Antp [ID 9ANT] homeodomain DNA structure)

## References

1. Krumlauf R (1994) *Hox* genes in vertebrate development. *Cell* 78:191–201
2. Capecchi MR (1997) *Hox* genes and mammalian development. *Cold Spring Harb Symp Quant Biol* 62:273–281
3. Scott MP (1993) A rational nomenclature for vertebrate homeobox (*HOX*) genes. *Nucleic Acids Res* 21:1687–1688
4. Akarsu AN, Stoilov I, Yilmaz E, Sayli BS, Sarfarazi M (1996) Genomic structure of *HOXD13* gene: a nine polyalanine duplication causes synpolydactyly in two unrelated families. *Hum Mol Genet* 5:945–952
5. Gehring WJ, Qian YQ, Billeter M, Furukubo-Tokunaga K, Schier AF, Resendez-Perez D, Affolter M, Otting G, Wüthrich K (1994) Homeodomain-DNA recognition. *Cell* 78:211–223
6. Kissinger CR, Liu BS, Martinblanco E, Kornberg TB, Pabo CO (1990) Crystal-structure of an engrailed homeodomain-DNA complex at 2.8 Å resolution: a framework for understanding homeodomain-DNA interaction. *Cell* 63:579–590
7. Fraenkel E, Rould MA, Chambers KA, Pabo CO (1998) Engrailed homeodomain-DNA complex at 2.2 Å resolution: a

- detailed view of the interface and comparison with other engrailed structure. *J Mol Biol* 284:351–361
8. Clarke ND, Kissinger CR, Desjarlais J, Gilliland GL, Pabo CO (1994) Structural studies of the engrailed homeodomain. *Protein Sci* 3:1779–1787
  9. Treisman J, Gonczy P, Vashishtha M, Harris E, Desplan C (1989) A single amino-acid can determine the DNA-binding specificity of homeodomain proteins. *Cell* 59:553–562
  10. Hanes SD, Brent R (1989) DNA specificity of the bicoid activator protein is determined by homeodomain recognition helix residue-9. *Cell* 57:1275–1283
  11. Goodman FR (2002) Limb malformations and the human *HOX* genes. *Am J Med Genet* 112:256–265
  12. Muragaki Y, Mundlos S, Upton J, Olsen BR (1996) Altered growth and branching patterns in synpolydactyly caused by mutations in *HOXD13*. *Science* 272:548–551
  13. Goodman FR, Mundlos S, Muragaki Y, Donnai D, Giovannucci-Uzielli ML, Lapi E, Majewski F, McGaughan J, McKeown C, Reardon W, et al (1997) Synpolydactyly phenotypes correlate with size of expansions in *HOXD13* polyalanine tract. *Proc Natl Acad Sci USA* 94:7458–7463
  14. Baffico M, Baldi M, Cassan PD, Costa M, Mantero R, Garani P, Camera G (1997) Synpolydactyly: clinical and molecular studies on four Italian families. *Eur J Hum Genet Suppl* 5: 142
  15. Kjaer KW, Hedeboe J, Bugge M, Hansen C, Friis-Henriksen K, Vestergaard MB, Tommerup N, Opitz JM (2002) *HOXD13* polyalanine tract expansion in classical synpolydactyly type Vordingborg. *Am J Med Genet* 110:116–121
  16. Kjaer KW, Hansen L, Eiberg H, Utkus A, Skovgaard LT, Leicht P, Opitz JM, Tommerup N (2005) A 72-year-old Danish puzzle resolved—comparative analysis of phenotypes in families with different-sized *HOXD13* polyalanine expansion. *Am J Med Genet A* 138:328–339
  17. Zhao XL, Meng JP, Sun M, Ao Y, Wu AH, Lo HY, Zhang X (2005) *HOXD13* polyalanine tract expansion in synpolydactyly: mutation detection and prenatal diagnosis in a large Chinese family. *Zhonghua Yi Xue Yi Chuan Xue Za Zhi* 22: 5–9
  18. Goodman FR, Giovannucci-Uzielli ML, Hall C, Reardon W, Winter R, Scambler P (1998) Deletions in *HOXD13* segregate with an identical, novel foot malformation in two unrelated families. *Am J Hum Genet* 63:992–1000
  19. Calabrese O, Bigoni S, Gualandi F, Trabanelli C, Camera G, Calzolari E (2000) A new mutation in *HOXD13* associated with foot pre-postaxial polydactyly. *Eur J Hum Genet Suppl* 8:140
  20. Kan SH, Johnson D, Giele H, Wilkie AO (2003) An acceptor splice site mutation in *HOXD13* results in variable hand, but consistent foot malformations. *Am J Med Genet A* 121:69–74
  21. Debeer P, Bacchelli C, Scambler PJ, De Smet L, Fryns JP, Goodman FR (2002) Severe digital abnormalities in a patient heterozygous for both a novel missense mutation in *HOXD13* and a polyalanine tract expansion in *HOXA13*. *J Med Genet* 39:852–856
  22. Johnson KR, Sweet HO, Donahue LR, Ward-Bailey P, Bronson RT, Davisson MT (1998) A new spontaneous mouse mutation of *Hoxd13* with a polyalanine expansion and phenotype similar to human synpolydactyly. *Hum Mol Genet* 7:1033–1038
  23. Albrecht AN, Schwabe GC, Stricker S, Boddrich A, Wanker EE, Mundlos S (2002) The synpolydactyly homolog (*spdh*) mutation in the mouse—a defect in patterning and growth of limb cartilage elements. *Mech Dev* 112:53–67
  24. Johnson D, Kan S-h, Oldridge M, Trembath RC, Roche P, Esnouf RM, Giele H, Wilkie AOM (2003) Missense mutations in the homeodomain of *HOXD13* are associated with brachydactyly types D and E. *Am J Hum Genet* 72:984–997
  25. Caronia G, Goodman FR, McKeown CME, Scambler PJ, Zappavigna V (2003) An I47L substitution in the *HOXD13* homeodomain causes a novel human limb malformation by producing a selective loss of function. *Development* 130:1701–1712
  26. Temtamy SA, McKusick VA (1978) Syndactyly. In: Bergsma (ed) *The genetics of hand malformations*. Alan R. Liss, New York, pp 301–322
  27. Malik S, Ahmad W, Grzeschik KH, Koch MC (2005) A simple method for characterizing syndactyly in clinical practice. *Genet Couns* 16:229–238
  28. Robinow M, Johnson GE, Brook GJ (1982) Syndactyly type V. *Am J Med Genet* 11:475–482
  29. Salsi V, Zappavigna V (2006) *Hoxd13* and *Hoxa13* directly control the expression of the *EphA7* ephrin tyrosine kinase receptor in developing limbs. *J Biol Chem* 281:1992–1999
  30. Fraenkel E, Pabo CO (1998) Comparison of X-ray and NMR structures for the *Antennapedia* homeodomain-DNA complex. *Nature Struct Biol* 5:692–697
  31. Kleywegt GJ, Jones TA (1996) Efficient rebuilding of protein structures. *Acta Crystallogr D Biol Crystallogr* 52:829–832
  32. Kalé L, Skeel R, Bhandarkar M, Brunner R, Gursoy A, Krawetz N, Phillips J, Shinozaki A, Varadarajan K, Schulten K (1999) NAMD2: greater scalability for parallel molecular dynamics. *J Comput Phys* 151:283–312
  33. MacKerell AD Jr, Bashford D, Bellott M, Dunbrack RL Jr, Evanseck JD, Field MJ, Fischer S, Gao J, Guo H, Ha S, et al (1998) All-atom empirical potential for molecular modeling and dynamics studies of proteins. *J Phys Chem B* 102:3586–3616
  34. Qian YQ, Otting G, Wüthrich K (1993) NMR1 detection of hydration water in the intermolecular interface of a protein-DNA complex. *J Am Chem Soc* 115:1189–1190
  35. Billeter M, Guntert P, Luglinbuhl P, Wüthrich K (1996) Hydration and DNA recognition by homeodomains. *Cell* 85:1057–1065
  36. Humphrey W, Dalke A, Schulten K (1996) VMD: visual molecular dynamics. *J Mol Graph* 14:33–38
  37. Baberjee-Basu S, Baxeavanis AD (2001) Molecular evolution of the homeodomain family of transcription factors. *Nucleic Acids Res* 29:3258–3269
  38. Brown LY, Brown SA (2004) Alanine tracts: the expanding story of human illness and trinucleotide repeats. *TIG* 20:51–58
  39. Amiel J, Trochet D, Clement-Ziza M, Munnich A, Lyonnet S (2004) Polyalanine expansions in human. *Hum Mol Genet* 13:R235–R243
  40. Albrecht A, Mundlos S (2005) The other trinucleotide repeat: polyalanine expansion disorders. *Curr Opin Genet Dev* 15: 285–293
  41. Warren ST (1997) Polyalanine expansion in synpolydactyly might result from unequal crossing-over of *HOXD13*. *Science* 275:408–409
  42. Dollé P, Duboule D (1989) Two gene members of the murine *HOX-5* complex show regional and cell-type specific expression in developing limbs and gonads. *EMBO J* 8:1507–1515
  43. Mortlock D, Sateesh P, Innis JW (2000) Evolution of N-ter-

- minal sequences of the vertebrate HOXA13 protein. *Mamm Genome* 11:151–158
44. Dollé P, Dierich A, LeMeur M, Schimmang T, Schuhbauer B, Chambon P, Duboule D (1993) Disruption of the *Hoxd13* gene induces localized heterochrony leading to mice with neotenic limbs. *Cell* 75:431–441
  45. Davis AP, Capecchi MR (1996) A mutational analysis of the 5' *HoxD* genes: dissection of genetic interactions during limb development in the mouse. *Development* 122:1175–1185
  46. Haga H, Yamada R, Ohnishi Y, Nakamura Y, Tanaka T (2002) Gene-based SNP discovery as part of the Japanese Millennium Genome Project: identification of 190,562 genetic variations in the human genome. *J Hum Genet* 47:605–610
  47. Lavoie H, Debeane F, Trinh QD, Turcotte JF, Corbeil-Girard LP, Dicaire MJ, Saint-Denis A, Page M, Rouleau GA, Brais B (2003) Polymorphism, shared functions and convergent evolution of genes with sequences coding for polyalanine domains. *Hum Mol Genet* 12:2967–2979
  48. Vargas AO, Fallon JF (2005) The digits of the wing of birds are 1, 2 and 3: a review. *J Exp Zool B Mol Dev Evol* 304:206–219
  49. David AP, Capecchi MR (1994) Axial homeosis and appendicular skeleton defects in mice with targeted disruption of *hoxd-11*. *Development* 120:2187–2198
  50. Zákány J, Duboule D (1996) Syndactyly in mice with a targeted deficiency in the *HoxD* complex. *Nature* 384:69–71
  51. Brudeau S, Johnson KR, Yamamoto M, Kuroiwa A, Duboule D (2001) The mouse *Hoxd13<sup>spd</sup>* mutation, a polyalanine expansion similar to human type II synpolydactyly (SPD), disrupts the function but not the expression of other *Hoxd* genes. *Dev Biol* 237:345–353
  52. Albrecht AN, Kornak U, Boddich A, Suring K, Robinson PN, Stiege AC, Lurz R, Stricker S, Wanker EE, Mundlos S (2004) A molecular pathogenesis for transcription factor associated poly-alanine tract expansions. *Hum Mol Genet* 13:2351–2359
  53. Mortlock DP, Innis JW (1997) Mutation of *HOXA13* in hand-foot-genital syndrome. *Nat Genet* 15:179–180
  54. Innis JW, Goodman FR, Bacchelli C, Williams TM, Mortlock DP, Sateesh P, Scambler PJ, McKinnon W, Guttmacher AE (2002) A HOXA13 allele with a missense mutation in the homeobox and a dinucleotide deletion in the promoter underlies Guttmacher syndrome. *Hum Mutat* 19:573–574
  55. Blondelle SE, Forood B, Houghten A, Perez-Paya E (1997) Polyalanine-based peptides as models for self-associated  $\beta$ -pleated-sheet complexes. *Biochemistry* 36:8393–8400